ORIGINAL ARTICLE

Large-effect loci affect survival in Tasmanian devils (*Sarcophilus harrisii*) infected with a transmissible cancer

Mark J. Margres[1,*] | Menna E. Jones[2,*] | Brendan Epstein[1,*] | Douglas H. Kerlin[3] | Sebastien Comte[2] | Samantha Fox[4] | Alexandra K. Fraik[1] | Sarah A. Hendricks[5] | Stewart Huxtable[4] | Shelly Lachish[6] | Billie Lazenby[4] | Sean M. O'Rourke[7] | Amanda R. Stahlke[5] | Cody G. Wiench[5] | Rodrigo Hamede[2,8] | Barbara Schönfeld[2] | Hamish McCallum[3] | Michael R. Miller[7] | Paul A. Hohenlohe[5] | Andrew Storfer[1]

[1]School of Biological Sciences, Washington State University, Pullman, Washington

[2]School of Zoology, University of Tasmania, Hobart, Tasmania, Australia

[3]School of Environment, Griffith University, Nathan, Queensland, Australia

[4]Save the Tasmanian Devil Program, Department of Primary Industries, Parks, Water and Environment, Hobart, Tasmania, Australia

[5]Department of Biological Sciences, Institute for Bioinformatics and Evolutionary Studies, University of Idaho, Moscow, Idaho

[6]Department of Zoology, University of Oxford, Oxford, UK

[7]Department of Animal Science, University of California, Davis, Davis, California

[8]Centre for Integrative Ecology, Deakin University, Waurn Ponds, Victoria, Australia

Correspondence
Andrew Storfer, School of Biological Sciences, Washington State University, Pullman, WA.
Email: astorfer@wsu.edu
and
Paul A. Hohenlohe, Department of Biological Sciences, Institute for Bioinformatics and Evolutionary Studies, University of Idaho, Moscow, ID.
Email: hohenlohe@uidaho.edu

Present address
Brendan Epstein, Department of Plant Biology, University of Minnesota, 250 Biosciences, St. Paul, Minnesota.

Abstract

Identifying the genetic architecture of complex phenotypes is a central goal of modern biology, particularly for disease-related traits. Genome-wide association methods are a classical approach for identifying the genomic basis of variation in disease phenotypes, but such analyses are particularly challenging in natural populations due to sample size difficulties. Extensive mark–recapture data, strong linkage disequilibrium and a lethal transmissible cancer make the Tasmanian devil (*Sarcophilus harrisii*) an ideal model for such an association study. We used a RAD-capture approach to genotype 624 devils at ~16,000 loci and then used association analyses to assess the heritability of three cancer-related phenotypes: infection case–control (where cases were infected devils and controls were devils that were never infected), age of first infection and survival following infection. The SNP array explained much of the phenotypic variance for female survival (>80%) and female case–control (>61%). We found that a few large-effect SNPs explained much of the variance for female survival (~5 SNPs explained >61% of the total variance), whereas more SNPs (~56) of smaller effect explained less of the variance for female case–control (~23% of the total variance). By contrast, these same SNPs did not account for a significant proportion of phenotypic variance in males, suggesting that the genetic bases of these traits and/or selection differ across sexes. Loci involved with cell adhesion and cell-cycle regulation underlay trait variation, suggesting that the devil immune system is rapidly evolving to recognize and potentially suppress cancer growth through these pathways. Overall, our study provided necessary data for genomics-based conservation and management in Tasmanian devils.

KEYWORDS
adaptation, cancer, effect size, genotype–phenotype, GWAS

1 | INTRODUCTION

A long-standing and significant problem in biology is understanding the genotype–phenotype relationship, and the recent development of genomic techniques has allowed researchers to address this problem with increasing sophistication. Because the genetic basis of polygenic traits, however, has been difficult to characterize, the genetics underlying many ecologically important and disease-related traits is often unknown (Savolainen, Lascoux, & Merilä, 2013; Schork et al., 2013; Shao et al., 2008; Wellenreuther & Hansson, 2016). To date, genome-wide association studies (GWASes) have largely been used to identify variants associated with complex phenotypes (Gibson, 2012; Manolio et al., 2009), particularly those related to disease. Although GWASes have successfully identified candidate loci, discovered variants often explain only a small proportion of the phenotypic variance (Eichler et al., 2010; Marjoram, Zubair, & Nuzhdin, 2014; Park et al., 2010; Schork et al., 2013) and, therefore, possess low predictive power (Chatterjee et al., 2013). Indeed, most variants in humans exhibit small effect sizes and explain only a small proportion of heritability (Hindorff et al., 2009; Yang et al., 2010, 2012) despite a bias towards detecting and publishing larger effect sizes (i.e., "Winner's Curse"; Dembeck et al., 2015; Gibson, 2012; Park et al., 2010).

A handful of studies have found evidence of large-effect SNPs for certain traits in humans (e.g., ~12 variants or fewer explained ~50% of the phenotypic variance), such as pigmentation (Sulem et al., 2007), age-related macular degeneration (Jakobsdottir, Gorin, Conley, Ferrell, & Weeks, 2009), hypoxia adaptation (Simonson et al., 2010), lung cancer risk (Wang et al., 2014) and lipid levels associated with coronary heart disease (Helgadottir et al., 2016). Other studies, however, have argued that the polygenic nature of complex traits often requires thousands of SNPs to explain a large proportion of the heritability; for example, ~9,500 variants explained ~50% of the variation in human height (Wood et al., 2014). Even in these case studies, much of the phenotypic variance is still unaccounted for (Yang et al., 2010, 2015). This missing heritability could be the result of many variants of small effect being missed due to significance thresholds, unsampled rare variants of large effect and/ or causal variants of any effect size not being captured by the SNP array (e.g., causal variants not being in linkage disequilibrium [LD] with the genotyped variants; Gibson, 2012; Hindorff et al., 2009; Manolio et al., 2009). Therefore, even in humans for which we have extensive genomic resources and genotypic information for millions of individuals, it remains unclear whether most quantitative traits are determined by many loci of small effect or a few loci of large effect.

Identifying the genetic basis of ecologically important traits in threatened and endangered wildlife populations is becoming increasingly important for management and conservation, such as to guide captive breeding programmes. Emerging infectious diseases (EIDs) are now considered a major cause of species' declines and endangerment, and GWAS methods are a classical approach for identifying the genomic basis of variation in disease phenotypes (e.g., Hindorff et al., 2009). GWASes in natural populations, however, are particularly challenging owing to difficulties in achieving sufficient sample sizes to attain appropriate statistical power (Kardos, Husby, McFarlane, Qvarnström, & Ellegren, 2016). For example, identifying the genetic basis of a complex trait such as survival following infection requires extensive mark–recapture data that are often difficult to obtain. As a result, the rare examples of large-effect loci in wildlife species (e.g., colour variation in mice; [Linnen et al., 2013] and armour plating in sticklebacks; [Colosimo et al., 2005]) have not typically been associated with disease and have been discovered using methods other than GWAS approaches. Although detecting variants of an appreciable effect in relatively large natural populations typically requires several thousand samples and extensive sampling of the genome (Yang et al., 2015), simulations have demonstrated that these variants can be reliably detected with far less sampling in relatively small populations with strong LD (e.g., LD >50 kb; Kardos et al., 2016). The Tasmanian devil (*Sarcophilus harrisii*) matches these criteria; with extensive mark–recapture field data, strong LD (~200 kb; Epstein et al., 2016), and a species-specific, nearly 100% lethal infectious cancer (Hamede et al., 2015), the devil is an ideal model for a GWAS in a natural population.

The Tasmanian devil is the largest extant marsupial carnivore, and facial tumours were first discovered in the northeastern part of the island in 1996. The disease is caused by an infectious cell line and is, therefore, a transmissible cancer (Pearse & Swift, 2006). Such cancers are extremely rare, with the only other natural cases found in dogs (Murgia, Pritchard, Kim, Fassati, & Weiss, 2006) and bivalves (Metzger et al., 2016). Since 1996, devil facial tumour disease (DFTD) has spread approximately 80% of the way across Tasmania, caused upwards of 95% declines in populations affected the longest and reduced the total population size by 80% (McCallum, 2008; McCallum et al., 2009). The cancer is spread via biting, which is common during social interactions (Hamede, McCallum, & Jones, 2013). Low genetic diversity in devils due to historic population bottlenecks (3–5 k years ago; Brüniche-Olsen, Jones, Austin, Burridge, & Holland, 2014; Hendricks et al., 2017; Miller et al., 2011) and silencing of cell surface MHC molecules by DFTD have led to what appears to be universal susceptibility (Siddle et al., 2013). Simple epidemiological models have predicted devil extinction 25–30 years following disease arrival (McCallum et al., 2009), but the longest-diseased populations persist, suggesting devils may be responding to the strong selection imposed by DFTD (Jones et al., 2008). Indeed, recent work has discovered that some devils exhibited an immune response to DFTD (Pye et al., 2016) and, in rare cases, even tumour regression (Wright et al., 2017). Further, time-series genome scan analyses across three populations pre- and post-DFTD emergence found evidence for rapid evolution in genes related to immune function and cancer risk (Epstein et al., 2016). Taken together, these results suggest the evolution of resistance and/or tolerance to DFTD.

Although genomic regions showing a signature of selection have been identified (Epstein et al., 2016), the relationship of these markers to specific DFTD-related phenotypes as well as effect sizes of particular variants is unknown. We used a restriction-site associated DNA (RAD)-capture ("Rapture") approach (Ali et al., 2016) to genotype 624 individuals from six localities (Figure 1) at approximately 16,000 RAD loci; loci were selected for homology with mammalian immune function, cancer recognition, and to provide broad coverage of the genome. We then used association analyses to assess heritability and identify loci underlying three devil phenotypes/phenotype proxies: infection case–control (where cases were infected devils and controls were devils that were never infected), age of first infection and survival following infection.

2 | MATERIALS AND METHODS

2.1 | Trapping and phenotypic data

Tasmanian devils were trapped from 2000 to 2016 using custom-built traps constructed of 300-mm polypropylene pipe. All traps were baited with meat. Trapping sessions were carried out with 40–120 traps over 7–10 consecutive nights in a capture–mark–recapture framework. Traps were checked daily beginning at dawn; details of field methods were previously described (Hamede et al., 2015). Following initial capture, devils were individually tagged with microchip
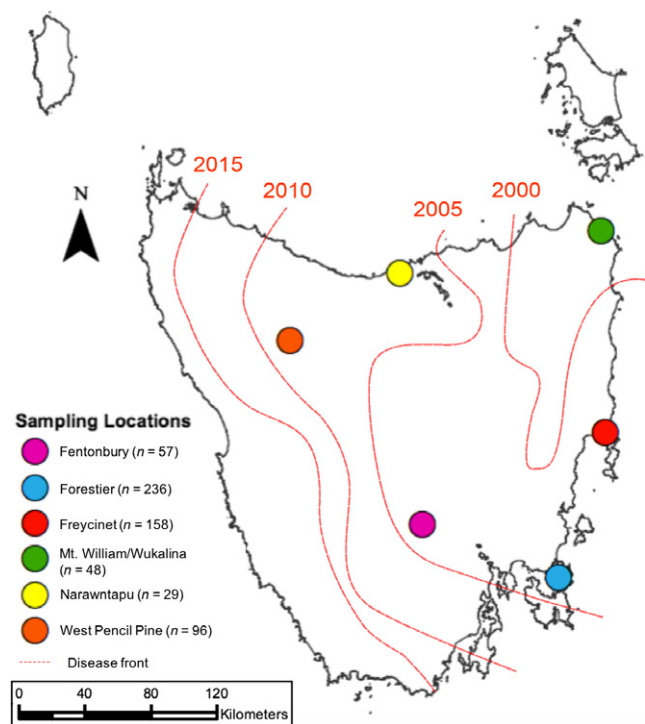

FIGURE 1 Sampling localities in Tasmania. We genotyped and phenotyped 624 Tasmanian devils from six collection sites. Red lines indicate the approximate location of the disease front from 2000 to 2015

transponders (Allflex NZ Ltd, Palmerstone North, New Zealand). Devils were aged using a combination of head width (a linear measure of body size), molar eruption, molar tooth wear and canine over-eruption. Most individuals were trapped as juveniles, and therefore, the age was known. DFTD status was categorized from histopathological confirmation of tumour biopsies. All devils were released following data collection (see below) except for nine devils from Forestier that were euthanized for health reasons; these devils were not included in survival analyses (see below), although their inclusion did not affect results (data not shown).

We performed association analyses (described below) for three phenotypes: (a) case–control where "cases" were infected individuals, and "controls" were individuals that were never infected and were captured (uninfected) ≥800 days from the estimated date of birth for the GEMMA analyses and ≥1,000 days for the ANGSD analysis (see below); (b) the estimated age of an individual (in days) when it was first observed with DFTD; and (c) length of known time to be alive (in days) after being observed with DFTD, our proxy for survival. Because observing the endpoint of death in a mark–recapture trapping framework is impossible (i.e., cannot trap a dead individual), we estimated survival as the difference in days between the first time an individual was observed with DFTD and the last time it was observed at all; we required at least two capture events following infection and that the individual must have survived ≥40 days to allow for recapture to be possible. We recognize that our survival estimate was a simplified proxy for true survival, but we did not

possess the necessary longitudinal data across all sampled sites to more robustly model true survival as previously described (Wells et al., 2017). Mark–recapture frameworks estimate survival for classes of individuals (e.g., McDonald, 2018), but individual phenotype estimates are required for GWASes. We therefore chose to maximize sample size and statistical power by using the simplified survival proxy described above. To complement this simplified survival metric, we calculated an additional estimate for a single sampling locality (West Pencil Pine) for which we possessed the necessary longitudinal data to do so. West Pencil Pine is the most intensely and consistently sampled locality and has been sampled at 3-month intervals since the outbreak of the disease in 2006. Additionally, tumour growth models and robust survival estimates (Hamede, Beeton, Carver, & Jones, 2017; Wells et al., 2017) have been calculated only for this locality. We used our individual tumour measurements and the logistic tumour growth curves from Wells et al. (2017) to back-calculate from the first observation of a tumour on an individual to the time when the tumour was at a volume of 3 mm^3 (representing the size at which tumours are first observable) for 60 individuals from West Pencil Pine. We then followed the approach of Kéry and Schaub (2011) to test for differences in recapture probabilities while controlling for infection status and seasonality. We did not detect any significant differences in recapture probabilities between seasons or disease status (data not shown). Therefore, any adjustments made to estimate survival beyond the last capture would be made equally to diseased (i.e., cases) and non-diseased (i.e., controls) individuals and would have no effect on the association analyses. The new West Pencil Pine-specific survival proxy was the time in days from the back-calculated date of infection to the date of final capture. We use "survival" to refer to the simplified proxy (i.e., the difference in days between the first time an individual was observed with DFTD and the last time it was observed at all) throughout the manuscript and "West Pencil Pine-specific survival" to refer to the back-calculated survival estimate for the 60 West Pencil Pine individuals. The simplified survival proxy and the West Pencil Pine-specific estimates showed a significant, positive correlation ($p < 0.0001$, $R^2 = 0.7117$, $R = 0.8050$; Supporting Information Figure S1), indicating that our simplified proxy provided a fair estimate of survival following infection. For age of first infection and case–control, we only included individuals that were born during or after the first year of DFTD in their respective population. Because the West Pencil Pine site was not strongly impacted by disease from 2006 to 2011 due to the presence of a tetraploid tumour associated with low prevalence rates (Hamede et al., 2015), we used 2011 as the year of disease arrival for this population. All phenotype data are provided in Supporting Information Table S1.

2.2 | RAD-capture array development

We used the data (i.e., 360 individuals sequenced for 90,000 loci) from Epstein et al. (2016) to develop a RAD-capture array (Ali et al., 2016); the details of data processing and genotyping of the original RAD loci have been previously described (Epstein et al., 2016).

RAD-capture extends traditional RADseq, which amplifies all loci adjacent to restriction enzyme cut sites, by adding a sequence capture step to the end of the RADseq protocol (Ali et al., 2016). We targeted 7,108 RAD loci that were genotyped in more than half the individuals, had ≤3 non-singleton SNPs and had a SNP with a minor allele frequency (MAF) ≥0.05. To improve coverage of the genome, each locus was ≥20 kb away from other targeted loci. Additionally, we targeted 6,315 loci that had a non-singleton SNP within 50 kb of an immune related gene, had ≤4 non-singleton SNPs and were genotyped in ≥1/3 of the individuals. Finally, we targeted 3,316 loci that showed some preliminary evidence of association with DFTD susceptibility and had ≤5 non-singleton SNPs (Epstein et al., 2016). In total, we targeted 15,898 RAD loci (there was some overlap among criteria). All targeted restriction cut sites are provided in Supporting Information Table S2.

2.3 | Sequencing and data processing

RAD-capture libraries were constructed using the *pstI* restriction enzyme for 624 *S. harrisii* from six localities (Figure 1). Libraries were sequenced on an Illumina NextSeq at the University of Oregon Genomics and Cell Characterization Core Facility. Reads were demultiplexed, and low-quality reads were removed using process_radtags from STACKS (version 1.21; Catchen, Hohenlohe, Bassham, Amores, & Cresko, 2013); this step also removed reads without recognizable barcodes or cut sites. The clone_filter program was used to remove potential PCR duplicates. Reads were then aligned to the reference genome (downloaded from Ensembl June 2014; Murchison et al., 2012) using bowtie2 (Langmead & Salzberg, 2012) with the --sensitive, --end-to-end, and -X 900 settings. Reads were retained if they aligned to an expected locus or were the mate of a read that aligned to an expected locus. Regions on the X chromosome were excluded from all analyses due to reduced genotyping accuracy and power (Wise, Gyi, & Manolio, 2013); only 350 of the 15,898 targets occurred on the X chromosome. Plots of number of loci covered per individual, number of individuals with coverage per locus and mean depth of coverage per individual are provided in Supporting Information Figure S2.

Because GEMMA association analyses (see below) required individual genotype calls, genotype likelihoods for each potential segregating position were calculated with ANGSD (described in detail below; Korneliussen, Albrechtsen, & Nielsen, 2014); missing genotypes were imputed, and genotype probabilities were calculated in BEAGLE (Howie, Donnelly, & Marchini, 2009). Imputation was conducted using a larger data set containing 3,568 individuals (data not shown), and each locality and chromosome was imputed separately; imputed genotypes are available upon request. The parameters and settings used in ANGSD (version 0.910) are provided in Supporting Information Table S3.

2.4 | GEMMA association tests

We fit a Bayesian Sparse Linear Mixed Model (BSLMM; Zhou, Carbonetto, & Stephens, 2013) implemented in GEMMA (Zhou &

Stephens, 2012) for case–control, age of first infection, survival following infection and the West Pencil Pine-specific survival estimate to characterize the genetic basis of each trait. Because preliminary models indicated a greater predictive power for some phenotypes when males and females were examined separately (data not shown), sexes were analysed collectively as well as independently. BSLMMs are a hybrid between linear mixed and sparse regression models and work under the assumption that most SNPs have a very small effect on the phenotype and a few SNPs have a larger effect. The model estimates an effect-size term for every SNP, the number of large-effect SNPs, the proportion of phenotypic variance explained by all SNPs (and other similar hyperparameters) and the proportion of phenotypic variance explained by only large-effect SNPs. The effect sizes are estimated simultaneously for all SNPs after accounting for relatedness via a K-matrix as well as background effects of all loci.

We used the imputed genotypes and genotype probabilities from BEAGLE (described above) as input for GEMMA. We ran GEMMA on SNPs with MAF >0.05 and ≤5% missing data following imputation. We ran ≥5 million iterations following a 500,000-iteration burn-in, and we chose the linear BSLMM option except for the case–control phenotype, for which we chose the probit model. Similar to previous work (Lind et al., 2017), we used the posterior probability of a SNP having a large effect on a phenotype (after accounting for the effects of other SNPs in the genome) to identify candidate genes (see below) because we felt that this metric aptly captured a variant's contribution to that particular trait. SNP counts and sample sizes are given in Table 1.

2.5 | Association tests with ANGSD

To complement our GEMMA analyses, we used ANGSD to run generalized linear model association tests (Skotte, Korneliussen, & Albrechtsen, 2012) on the same phenotypes described above except for the West Pencil Pine-specific survival estimate (not analysed in ANGSD). Although ANGSD does not calculate chip heritability and other genetic architecture statistics (e.g., effect size) as the BSLMM in GEMMA does, ANGSD directly incorporates genotyping uncertainty into the analysis by estimating the posterior probability of each possible genotype (using estimates of the population allele frequency); the generalized linear models used to test for an association between genotype and phenotype are summed over the possible genotypes and weighted by the posterior probabilities. ANGSD also directly calculates p-values for each per-SNP association whereas GEMMA does not. The same settings used for the allele frequency estimation were used here (Supporting Information Table S3). We used an additive association model and estimated the genotype probability using the allele frequency as a prior. Only sites with MAF ≥5% (as estimated by ANGSD) were included.

Sex was included as a covariate for all analyses. For the survival proxy, we also used age at first infection as a covariate. Because population structure can lead to inflated p-values in association testing (Xu & Shete, 2005), we conducted a PCA on genotypes and included principal component (PC) axes as covariates in the analyses. First, we obtained a genetic covariance matrix from the genotype likelihoods using ngsCovar (Fumagalli, Vieira, Linderoth, & Nielsen, 2014) and extracted the PCs. We next calculated Tracy–Widom significance values for the PCs (Patterson, Price, & Reich, 2006). Except for the survival phenotype (Pearson's correlation between first PC and phenotype; $p = 0.04$), PCs were not significantly correlated with phenotypes. For completeness, we ran the association analysis for each phenotype with no PCs and with a number of PCs chosen based on the appearance of scree plots (1–7, depending on the phenotype). We found that, without including any PCs, age at first infection exhibited a low inflation factor (1.02), and the QQ plot indicated a nearly flat distribution of p-values (Supporting Information Figure S3). For the case–control analysis, there was some inflation (inflation factor = 1.21), but including PCs resulted in little improvement in the inflation factor or the shape of the curve (inflation factor with PCs ranged from 1.18 to 2.18; Supporting Information Figure S3). For survival after infection, however, there was a clear improvement by including five PCs as covariates (Supporting Information Figure S3). Visualization of QQ plots was achieved using the qqman R package (Turner, 2014).

Following the recommendations of François, Martins, Caye, and Schoville (2016), we adjusted the p-values of ANGSD results based on a genomic inflation factor correction. The genomic inflation factor is the ratio between the median Z-scores and the expected median Z-scores for a χ^2 distribution with one degree of freedom (Devlin & Roeder, 1999), and works under the assumption that most SNPs are not strongly associated with the phenotype of interest. To perform the adjustment, we divided the raw Z-scores by the inflation factor. All p-values were adjusted before using them to identify candidate genes (Supporting Information Figure S4).

TABLE 1 Number of SNPs and individuals included for each association test

Analysis	SNPs	Samples
GEMMA: age at infection	10,777 (males)	213 (males)
	11,503 (females)	205 (females)
	10,569 (both)	418 (both)
GEMMA: case–control	10,777 (males)	275 (males)
	11,503 (females)	289 (females)
	10,461 (both)	564 (both)
GEMMA: survival after infection	10,777 (males)	41 (males)
	11,503 (females)	69 (females)
	11,875 (both)	110 (both)
ANGSD: age at infection	11,417	418
ANGSD: case–control	11,964	468
ANGSD: survival after infection	5,428	110

Notes. Because different numbers of capture events were required for each phenotype, sample sizes vary by trait. Because sample sizes vary by trait, SNP filtering, particularly filtering for minor allele frequency, varied by trait, resulting in different numbers of SNPs for each analysis within a phenotype.

2.6 | Identification of candidate genes

Candidate SNPs were identified as the top 0.1% of SNPs for each phenotype. Tasmanian devil genomes have extensive LD (~200 kb; Epstein et al., 2016), and we used bedtools (Quinlan & Hall, 2010) to conservatively identify candidate genes within 100 kb of the top SNPs. Putative gene functions were identified using GeneCards (www.genecards.org) and/or NCBI.

3 | RESULTS

3.1 | The genetic basis of cancer-resistant phenotypes

We first conducted joint-sex association tests using a BSLMM in GEMMA and found that the mean of the posterior distribution of the proportion of phenotypic variance explained (PVE; a measure of the additive effect of all interrogated SNPs, or "chip heritability"; Zhou et al., 2013) accounted for a substantial proportion of the variance for survival following infection (0.709; 95% CI = 0.276–0.999; Table 2). The survival proxy (the length of time known to be alive after being observed with DFTD) was associated with a few SNPs of large effect (~7), and these SNPs accounted for 60.6% of the PVE accounted for by all SNPs (or ~43% of the total PVE; Table 2). Mean PVE was less in the case–control phenotype (0.263; 95% CI = 0.088–0.502; Table 2), and this trait was associated with more SNPs of smaller effect (~63; Table 2). PVE credible intervals were large and approximately overlapped zero for age at first infection (Table 2). Although mean PVE was large for the West Pencil Pine-specific survival estimate (0.537), PVE credible intervals were also large (95% CI = 0.020–0.998; Supporting Information Figure S5 and Table S4).

Because preliminary models indicated a greater predictive power for some phenotypes when males and females were examined separately, we next conducted sex-specific association tests using a BSLMM in GEMMA and found that the mean PVE was substantial for female case–control (0.614; 95% CI = 0.214–0.984) and female survival following infection (0.801; 95% CI = 0.467–0.999; Figure 2; Table 2). Female survival was found to be associated with a few SNPs of large effect (~5; Table 2); these SNPs accounted for 76.5% of the PVE accounted for by all SNPs (e.g., five SNPs associated with female survival explained 76.5% of the 80.1% total PVE explained by all SNPs, or ~61% of the total PVE). Female case–control was associated with more SNPs of smaller effect (~56 SNPs accounted for ~23% of the total PVE; Table 2). PVE credible intervals were large and overlapped zero (or nearly so) for all traits in males (including survival following infection) as well as age of first infection in females (Figure 2; Table 2), potentially owing to small sample sizes and other confounding factors (Table 1; see Section 4 for detail). The large PVE credible intervals for male survival and male case–control, however, indicated that the substantial amount of variance explained in the initial joint-sex association tests for survival and, to a lesser extent, case–control, were driven by females. Consistent

with the joint-sex analyses above, mean PVE as well as PVE credible intervals was large for the West Pencil Pine-specific survival estimate in females (0.682, 95% CI = 0.052–0.999) and males (0.494, 95% CI = 0.015–0.998; Supporting Information Figure S5 and Table S4), suggesting that our simplified survival proxy was necessary to achieve greater sample sizes and, therefore, power for our association analyses.

3.2 | Cancer-resistant candidate genes

To determine which specific loci were associated with female survival and female case–control, we identified genes within 100 kb of the top 0.1% of SNPs from the GEMMA analyses, given that LD is strong at this scale within the genome (i.e., ~200 kb; Epstein et al., 2016); this approach identified candidate genes linked to variants with the largest effect for each trait. For female case–control, nine genes were identified within 100 kb of a top SNP, and five of these genes had putative functions; one gene, secretory carrier membrane protein 1, is implicated in immune function (Table 3). The largest posterior probability of any top SNP being of large effect was 0.193 and shared across four genes, again indicating that female case–control was associated with more SNPs of smaller effect (Supporting Information Table S5). Eight genes were within 100 kb of a top SNP related to female survival, and two of these genes had putative functions; one gene, ST8 alpha-N-acetyl-neuraminide alpha-2,8-sialyltransferase 2 (*ST8SIA2*), is implicated in immune function. *ST8SIA2* is related to chronic inflammation following infection and possessed the largest posterior probability of being a large-effect SNP for female survival (0.995; Supporting Information Table S5).

For the four phenotypes for which the PVE credible intervals approximately overlapped zero (all three traits in males and female age at first infection), all SNPs exhibited posterior probabilities of being a large-effect SNP ≤0.034, except for male age at first infection (≤0.069). Similarly, all SNPs associated with West Pencil Pine-specific survival exhibited posterior probabilities of being a large-effect SNP ≤0.018 for females and ≤0.056 for males. All posteriors for SNPs associated with these traits were substantially lower than those found for the two female phenotypes discussed above, indicating that the posterior probability of being a large-effect SNP reflected a variant's "significance" to a particular phenotype.

To complement the GEMMA results described above, we identified candidate genes within 100 kb of the top 0.1% of the SNPs identified in the ANGSD analyses for survival, age at first infection and case–control (Supporting Information Table S5). For case–control, 17 genes were identified within 100 kb of a top SNP, and 15 of these genes had putative functions. Nine of these genes are implicated in immune/tumour function and are listed in Supporting Information Table S5; candidates included genes involved with apoptosis (e.g., ADAMTS-like 4 [$p < 0.0001$], myeloid cell leukaemia 1 [$p < 0.0001$]), cell adhesion and signalling (integrin alpha 10 [$p = 0.0021$]) and non-self DNA recognition (RNA Polymerase III Subunit C [$p = 0.0021$]). For survival following infection, five genes were identified within 100 kb of a top SNP (Supporting Information Table S5). Four of

TABLE 2 GEMMA association results and genetic architecture statistics

Sex	Phenotype	Mean variance explained by all genotypes (%)	Median variance explained by all genotypes (%)	Number large-effect SNPs	Mean variance explained by large-effect SNPs (%)
Both	Age at infection	7.1 (0.3–21.6)	5.7	50.0 (0–270)	39.1 (0–96.2)
Both	Case–control	26.3 (8.8–50.2)	25.1	63.3 (0–269)	37.2 (0–96.1)
Both	Survival after infection	70.9 (27.6–99.9)	73.3	7.0 (1–34)	60.6 (26.2–97.3)
Female	Age at infection	16.1 (0.9–47.1)	13.1	38.1 (0–203)	36.5 (0–95.5)
Female	Case–control	61.4 (21.4–98.4)	61.3	56.1 (0–261)	38.3 (0–95.6)
Female	Survival after infection	80.1 (46.7–99.9)	82.4	4.8 (1–14)	76.5 (43.3–98.6)
Male	Age at infection	13.3 (0.4–42.5)	10.2	44.1 (0–246)	42.0 (0–96.4)
Male	Case–control	23.0 (1.4–64.9)	19.4	52.7 (0–261)	39.6 (0–96.3)
Male	Survival after infection	44.8 (1.1–99.6)	39.2	37.0 (0–196)	43.4 (0–96.6)

Notes. The mean variance explained by all genotypes represents the mean of the posterior distribution of the proportion of phenotypic variance explained. The mean variance explained by large-effect SNPs represents the percentage of the total variance explained by only large-effect SNPs (e.g., large-effect SNPs associated with female age at first infection explained 36.5% of the 16.1% total variance explained by all SNPs, or approximately 5.9% of the total variance). Parentheses present 95% posterior credible intervals from the posterior distributions.
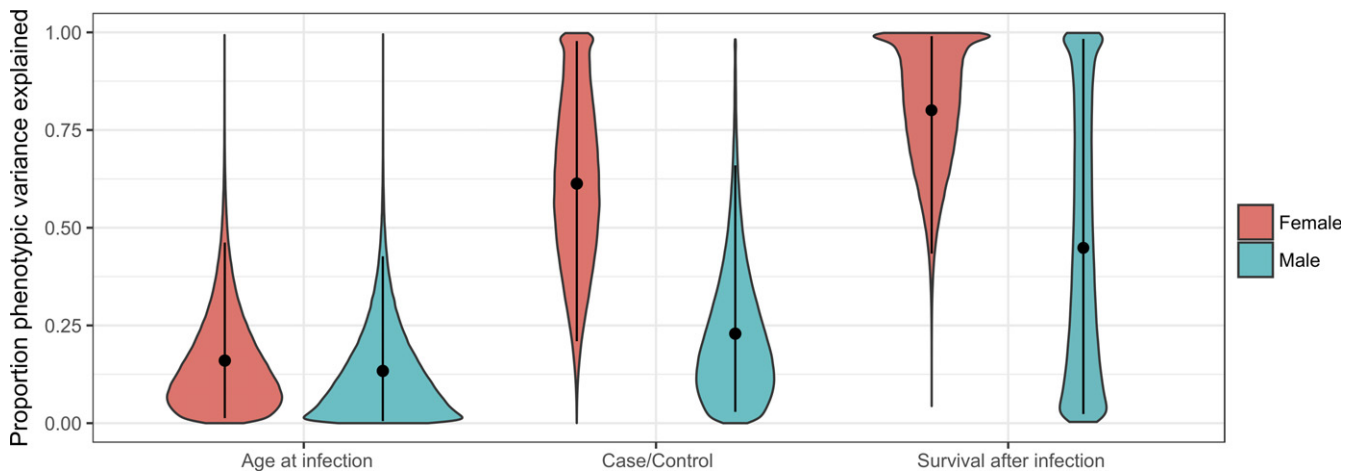

FIGURE 2 The proportion of the phenotypic variance explained by all sequenced genotypes for three disease-related traits. We plotted the GEMMA posterior distribution of the proportion of phenotypic variance explained by all SNPs (y-axis) for each phenotype (x-axis) for females (pink) and males (blue) independently. Points indicate the mean of the distribution, and bars represent 95% posterior credible intervals

these genes had putative functions, but none were implicated in immune and/or tumour function. For age at first infection, we identified nine genes within 100 kb of a top SNP (Supporting Information Table S5), and seven of these genes had putative functions. Four of these genes were implicated in immune/tumour function.

The top 1% of SNPs (and corresponding genes and statistics) from the nine GEMMA analyses and three ANGSD analyses are provided in Supporting Information Table S5; the top SNPs for the West Pencil Pine-specific survival estimate are not included.

4 | DISCUSSION

We identified the genetic basis underlying key cancer-resistant/tolerant phenotypes in Tasmanian devils and found that few loci of large effect explained a large proportion of the phenotypic variance for female survival. Female case–control was associated with more SNPs

of smaller effect, although relatively few loci (56 rather than thousands of variants) still accounted for a substantial amount of the total variance (23%; all genotypes accounted for 61.4%). Given the recent discovery of DFTD and subsequent evidence for a rapid evolutionary response in devils (approximately 4–6 generations; Epstein et al., 2016), we might expect that selection acted on standing genetic variation in the form of a few, large-effect loci. First-step (i.e., initial) mutations are often of large effect and confer a large fitness advantage because these mutations outcompete other, less beneficial mutations in the population (Rokyta, Joyce, Caudle, & Wichman, 2005), especially when the population is far from the phenotypic optimum as would be expected when selection is imposed by a novel disease. Novel beneficial mutations are unlikely to arise over short timescales, but large-effect variants can be segregating in the population neutrally prior to the onset of novel selective pressures (i.e., prior to DFTD arrival). Our results, at least for female survival, were consistent with these expectations. In contrast, PVE

TABLE 3 Candidate genes within 100 kb of the top 0.1% SNPs for female case–control and female survival following infection

Ensembl ID	Gene name	Putative function
Female case–control		
ENSSHAG00000011304	Forkhead box G1	Repressor
ENSSHAG00000001038	A kinase (PRKA) anchor protein 10	Binds to regulatory subunits of proteinase K
ENSSHAG00000003186	Unc-51 like autophagy activating kinase 2	Autophagy
ENSSHAG00000016943*	Secretory carrier membrane protein 1*	Recycling carrier to cell surface; implicated in immune function*
ENSSHAG00000017224	Adaptor-related protein complex 3, beta 1 subunit	Organelle biogenesis
Female survival after infection		
ENSSHAG00000010546*	ST8 alpha-*N*-acetyl-neuraminide alpha-2,8-sialyltransferase 2*	Catalyses sialic acid transfer; related to chronic inflammation due to infection*
ENSSHAG00000013531	Solute carrier family 12, member 8	Cation/chloride cotransporter

Notes. Only genes with a putative function were included. Genes with functions related to immune response and/or cancer risk were indicated with an asterisk.

confidence intervals approximately overlapped zero for all three traits in males and age of first infection in females.

A smaller male sample size for survival (41 males vs. 69 females; Table 1) suggested that a lack of power for the male survival association test may explain this sex-specific difference. However, similar sample sizes among sexes for case–control (275 males at 10,777 SNPs vs. 289 females at 11,503 SNPs) suggested that the difference in case–control PVE across males and females was biological rather than an artefact of our sampling. Whether this difference in case–control PVE represents a difference in genomic architecture and/or DFTD-imposed selection strength (e.g., due to differences in fecundity or other life history traits) across males and females remains uncertain. Sex chromosomes offer one possible molecular mechanism underlying this case–control difference. Sex chromosomes can enable the rapid evolution of sexual dimorphism, and both the Y chromosome (Kutch & Fedorka, 2015) and the inactivated X chromosome in females (Wang et al., 2016) have been shown to influence genome-wide expression, particularly for loci with an immune-related function. Kutch and Fedorka (2017) recently detected significant Y-chromosome-by-genetic-background epistatic effects following infection, including evidence of sign epistasis (i.e., reversal of fitness values). If a beneficial female allele is deleterious in males for a shared trait such as case–control, the trait heritability in males could be significantly reduced, consistent with our results. Additionally, males may experience different selective regimes than females because of higher variance in reproductive success, reducing the segregating genetic variation for male-expressed, DFTD-related traits. Further work is needed to test these hypotheses and identify the mechanism underlying the sex-based differences in PVE we identified in this study.

Prior work showed a rapid evolutionary response in two small genomic regions on chromosomes 3 and 4 in genes associated with cell-cycle regulation, cell adhesion and immune response (Epstein et al., 2016), but the relationship of these genomic regions to specific phenotypes was unknown. Consistent with this previous work, we found that loci involved with immunity, cell-cycle regulation and cell adhesion underlay variation in female survival and may thereby drive cancer resistance (or tolerance; Wells et al., 2017). For example, Epstein et al. (2016) identified *CD146* as a candidate gene, and we identified *ST8SIA2* as a top candidate gene associated with female survival. Both of these genes are involved with cell adhesion and often regulate inflammatory response. Collectively, the functions of these candidate genes, along with the phenotypes they are associated with, indicate that the devil immune system is evolving to recognize, and potentially suppress, the growth of tumour cells, providing a potential mechanism for the recently identified tumour regression in specific devil populations (Wright et al., 2017).

As global biodiversity is increasingly threatened by anthropogenically driven changes such as EIDs, effective conservation management will likely benefit from an understanding of the genomic signatures of adaptation in natural populations. Here, we showed that genomic studies can be applied to natural populations to guide conservation and management. We found that few loci of large effect explain variation in survival in the face of a lethal EID. In such cases, clear management recommendations emerge, such as basing the selection of individuals for captive breeding programmes on this genetic information to ensure the survival of the Tasmanian devil. Discovery of EIDs continues to increase and, together with predictions of rapid and dramatic global change, will necessitate rapid responses in terms of conservation and management.

DATA ACCESSIBILITY

The sequence data have been deposited at NCBI under BioProject PRJNA306495 (http://www.ncbi.nlm.nih.gov/bioproject/?term=PRJNA306495); BioSample accessions are provided in Table S6. All phenotypic data are provided in Supporting Information Table S1.

AUTHOR CONTRIBUTIONS

M.J.M. analysed data and wrote the paper; M.E.J. oversaw collection of samples and phenotypic data; B.E. assisted in generating genomic data, analysed data and helped write the paper; D.K. generated and analysed data; S.C., S.F., S.H., S.L. and B.L. collected samples; A.K.F. assisted in data analysis and figure production; S.A.H. and S.M.O. assisted in generating genomic data; A.R.S. assisted in data analysis; C.G.W. assisted in generating genomic data; R.H. collected and collated phenotypic data and assisted in data analysis; B.S. assisted in generating genomic data; H.M. assisted in study design and data analysis; M.R.M. assisted in generating genomic data; P.A.H. oversaw genomic data production and bioinformatics; A.S. directed the project and helped write the paper.

ORCID

Mark J. Margres [ID] http://orcid.org/0000-0002-6153-6701
Alexandra K. Fraik [ID] http://orcid.org/0000-0002-9285-1173

REFERENCES

Ali, O. A., O'Rourke, S. M., Amish, S. J., Meek, M. H., Luikart, G., Jeffres, C., & Miller, M. R. (2016). RAD capture (Rapture): Flexible and efficient sequence-based genotyping. *Genetics*, *202*(2), 389–400. https://doi.org/10.1534/genetics.115.183665

Brüniche-Olsen, A., Jones, M. E., Austin, J. J., Burridge, C. P., & Holland, B. R. (2014). Extensive population decline in the Tasmanian devil predates European settlement and devil facial tumour disease. *Biology Letters*, *10*(11), 20140619. https://doi.org/10.1098/rsbl.2014.0619

Catchen, J., Hohenlohe, P. A., Bassham, S., Amores, A., & Cresko, W. A. (2013). Stacks: An analysis tool set for population genomics. *Molecular Ecology*, *22*(11), 3124–3140. https://doi.org/10.1111/mec.12354

Chatterjee, N., Wheeler, B., Sampson, J., Hartge, P., Chanock, S. J., & Park, J. H. (2013). Projecting the performance of risk prediction based on polygenic analyses of genome-wide association studies. *Nature Genetics*, *45*(4), 400–405. https://doi.org/10.1038/ng.2579

Colosimo, P. F., Hosemann, K. E., Balabhadra, S., Villarreal, G., Dickson, M., Grimwood, J., … Kingsley, D. M. (2005). Widespread parallel evolution in sticklebacks by repeated fixation of ectodysplasin alleles. *Science*, *307*(5717), 1928–1933. https://doi.org/10.1126/science.1107239

Dembeck, L. M., Huang, W., Magwire, M. M., Lawrence, F., Lyman, R. F., & Mackay, T. F. (2015). Genetic architecture of abdominal pigmentation in *Drosophila melanogaster*. *PLoS Genetics*, *11*(5), e1005163. https://doi.org/10.1371/journal.pgen.1005163

Devlin, B., & Roeder, K. (1999). Genomic control for association studies. *Biometrics*, *55*(4), 997–1004. https://doi.org/10.1111/j.0006-341X.1999.00997.x

Eichler, E. E., Flint, J., Gibson, G., Kong, A., Leal, S. M., Moore, J. H., & Nadeau, J. H. (2010). Missing heritability and strategies for finding the underlying causes of complex disease. *Nature Reviews Genetics*, *11*(6), 446. https://doi.org/10.1038/nrg2809

Epstein, B., Jones, M., Hamede, R., Hendricks, S., McCallum, H., Murchison, E. P., … Storfer, A. (2016). Rapid evolutionary response to a transmissible cancer in Tasmanian devils. *Nature Communications*, *7*, 12684. https://doi.org/10.1038/ncomms12684

François, O., Martins, H., Caye, K., & Schoville, S. D. (2016). Controlling false discoveries in genome scans for selection. *Molecular Ecology*, *25*(2), 454–469. https://doi.org/10.1111/mec.13513

Fumagalli, M., Vieira, F. G., Linderoth, T., & Nielsen, R. (2014). ngsTools: Methods for population genetics analyses from next-generation sequencing data. *Bioinformatics*, *30*(10), 1486–1487. https://doi.org/10.1093/bioinformatics/btu041

Gibson, G. (2012). Rare and common variants: Twenty arguments. *Nature Reviews Genetics*, *13*(2), 135–145. https://doi.org/10.1038/nrg3118

Hamede, R. K., Beeton, N. J., Carver, S., & Jones, M. E. (2017). Untangling the model muddle: Empirical tumour growth in Tasmanian devil facial tumour disease. *Scientific Reports*, *7*(1), 6217. https://doi.org/10.1038/s41598-017-06166-3

Hamede, R. K., McCallum, H., & Jones, M. (2013). Biting injuries and transmission of Tasmanian devil facial tumour disease. *Journal of Animal Ecology*, *82*(1), 182–190. https://doi.org/10.1111/j.1365-2656.2012.02025.x

Hamede, R. K., Pearse, A. M., Swift, K., Barmuta, L. A., Murchison, E. P., & Jones, M. E. (2015). Transmissible cancer in Tasmanian devils: Localized lineage replacement and host population response. *Proceedings of the Royal Society B: Biological Sciences*, *282*, 20151468. https://doi.org/10.1098/rspb.2015.1468

Helgadottir, A., Gretarsdottir, S., Thorleifsson, G., Hjartarson, E., Sigurdsson, A., Magnusdottir, A., … Sveinbjornsson, G. (2016). Variants with large effects on blood lipids and the role of cholesterol and triglycerides in coronary disease. *Nature Genetics*, *48*(6), 634–639. https://doi.org/10.1038/ng.3561

Hendricks, S., Epstein, B., Schönfeld, B., Wiench, C., Hamede, R., Jones, M., … Hohenlohe, P. (2017). Conservation implications of limited genetic diversity and population structure in Tasmanian devils (*Sarcophilus harrisii*). *Conservation Genetics*, *18*(4), 977–982. https://doi.org/10.1007/s10592-017-0939-5

Hindorff, L. A., Sethupathy, P., Junkins, H. A., Ramos, E. M., Mehta, J. P., Collins, F. S., & Manolio, T. A. (2009). Potential etiologic and functional implications of genome-wide association loci for human diseases and traits. *Proceedings of the National Academy of Sciences*, *106*(23), 9362–9367. https://doi.org/10.1073/pnas.0903103106

Howie, B. N., Donnelly, P., & Marchini, J. (2009). A flexible and accurate genotype imputation method for the next generation of genome-wide association studies. *PLoS Genetics*, 5(6), e1000529.

Jakobsdottir, J., Gorin, M. B., Conley, Y. P., Ferrell, R. E., & Weeks, D. E. (2009). Interpretation of genetic association studies: Markers with replicated highly significant odds ratios may be poor classifiers. *PLoS Genetics*, 5(2), e1000337.

Jones, M. E., Cockburn, A., Hamede, R., Hawkins, C., Hesterman, H., Lachish, S., … Pemberton, D. (2008). Life-history change in disease-ravaged Tasmanian devil populations. *Proceedings of the National Academy of Sciences*, 105(29), 10023–10027. https://doi.org/10.1073/pnas.0711236105

Kardos, M., Husby, A., McFarlane, S. E., Qvarnström, A., & Ellegren, H. (2016). Whole-genome resequencing of extreme phenotypes in collared flycatchers highlights the difficulty of detecting quantitative trait loci in natural populations. *Molecular Ecology Resources*, 16(3), 727–741. https://doi.org/10.1111/1755-0998.12498

Kéry, M., & Schaub, M. (2011). *Bayesian population analysis using WinBUGS: A hierarchical perspective*. Burlington, MA: Academic Press.

Korneliussen, T. S., Albrechtsen, A., & Nielsen, R. (2014). ANGSD: Analysis of next generation sequencing data. *BMC Bioinformatics*, 15(1), 356. https://doi.org/10.1186/s12859-014-0356-4

Kutch, I. C., & Fedorka, K. M. (2015). Y-linked variation for autosomal immune gene regulation has the potential to shape sexually dimorphic immunity. *Proceedings of the Royal Society B: Biological Sciences.*, 282, 20151301. https://doi.org/10.1098/rspb.2015.1301

Kutch, I. C., & Fedorka, K. M. (2017). A test for Y-linked additive and epistatic effects on surviving bacterial infections in *Drosophila melanogaster*. *Journal of Evolutionary Biology*, 30, 1400–1408. https://doi.org/10.1111/jeb.13118

Langmead, B., & Salzberg, S. L. (2012). Fast gapped-read alignment with Bowtie 2. *Nature Methods*, 9(4), 357–359. https://doi.org/10.1038/nmeth.1923

Lind, B. M., Friedline, C. J., Wegrzyn, J. L., Maloney, P. E., Vogler, D. R., Neale, D. B., & Eckert, A. J. (2017). Water availability drives signatures of local adaptation in whitebark pine (*Pinus albicaulis* Engelm.) across fine spatial scales of the Lake Taho Basin, USA. *Molecular Ecology*, 26(12), 3168–3185. https://doi.org/10.1111/mec.14106

Linnen, C. R., Poh, Y. P., Peterson, B. K., Barrett, R. D., Larson, J. G., Jensen, J. D., & Hoekstra, H. E. (2013). Adaptive evolution of multiple traits through multiple mutations at a single gene. *Science*, 339(6125), 1312–1316. https://doi.org/10.1126/science.1233213

Manolio, T. A., Collins, F. S., Cox, N. J., Goldstein, D. B., Hindorff, L. A., Hunter, D. J., … Cho, J. H. (2009). Finding the missing heritability of complex diseases. *Nature*, 461(7265), 747–753. https://doi.org/10.1038/nature08494

Marjoram, P., Zubair, A., & Nuzhdin, S. V. (2014). Post-GWAS: Where next? More samples, more SNPs or more biology? *Heredity*, 112(1), 79–88. https://doi.org/10.1038/hdy.2013.52

McCallum, H. (2008). Tasmanian devil facial tumour disease: Lessons for conservation biology. *Trends in Ecology and Evolution*, 23(11), 631–637. https://doi.org/10.1016/j.tree.2008.07.001

McCallum, H., Jones, M., Hawkins, C., Hamede, R., Lachish, S., Sinn, D. L., … Lazenby, B. (2009). Transmission dynamics of Tasmanian devil facial tumor disease may lead to disease-induced extinction. *Ecology*, 90(12), 3379–3392. https://doi.org/10.1890/08-1763.1

McDonald, T. (2018). *mra: Mark-Recapture Analysis*. R Package version 2.16.11. Retrieved from https://CRAN.R-project.org/package=mra

Metzger, M. J., Villalba, A., Carballal, M. J., Iglesias, D., Sherry, J., Reinisch, C., … Goff, S. P. (2016). Widespread transmission of independent cancer lineages within multiple bivalve species. *Nature*, 534(7609), 705–709. https://doi.org/10.1038/nature18599

Miller, W., Hayes, V. M., Ratan, A., Petersen, D. C., Wittekindt, N. E., Miller, J., … Wang, Q. (2011). Genetic diversity and population structure of the endangered marsupial *Sarcophilus harrisii* (Tasmanian devil). *Proceedings of the National Academy of Sciences*, 108(30), 12348–12353. https://doi.org/10.1073/pnas.1102838108

Murchison, E. P., Schulz-Trieglaff, O. B., Ning, Z., Alexandrov, L. B., Bauer, M. J., Fu, B., … Ng, B. L. (2012). Genome sequencing and analysis of the Tasmanian devil and its transmissible cancer. *Cell*, 148(4), 780–791. https://doi.org/10.1016/j.cell.2011.11.065

Murgia, C., Pritchard, J. K., Kim, S. Y., Fassati, A., & Weiss, R. A. (2006). Clonal origin and evolution of a transmissible cancer. *Cell*, 126(3), 477–487. https://doi.org/10.1016/j.cell.2006.05.051

Park, J. H., Wacholder, S., Gail, M. H., Peters, U., Jacobs, K. B., Chanock, S. J., & Chatterjee, N. (2010). Estimation of effect size distribution from genome-wide association studies and implications for future discoveries. *Nature Genetics*, 42(7), 570–575. https://doi.org/10.1038/ng.610

Patterson, N., Price, A. L., & Reich, D. (2006). Population structure and eigenanalysis. *PLoS Genetics*, 2(12), e190. https://doi.org/10.1371/journal.pgen.0020190

Pearse, A. M., & Swift, K. (2006). Allograft theory: Transmission of devil facial-tumour disease. *Nature*, 439(7076), 549. https://doi.org/10.1038/439549a

Pye, R. J., Pemberton, D., Tovar, C., Tubio, J. M., Dun, K. A., Fox, S., … Siddle, H. V. (2016). A second transmissible cancer in Tasmanian devils. *Proceedings of the National Academy of Sciences*, 113(2), 374–379. https://doi.org/10.1073/pnas.1519691113

Quinlan, A. R., & Hall, I. M. (2010). BEDTools: A flexible suite of utilities for comparing genomic features. *Bioinformatics*, 26(6), 841–842. https://doi.org/10.1093/bioinformatics/btq033

Rokyta, D. R., Joyce, P., Caudle, S. B., & Wichman, H. A. (2005). An empirical test of the mutational landscape model of adaptation using a single-stranded DNA virus. *Nature Genetics*, 37(4), 441. https://doi.org/10.1038/ng1535

Savolainen, O., Lascoux, M., & Merilä, J. (2013). Ecological genomics of local adaptation. *Nature Reviews Genetics*, 14(11), 807–820. https://doi.org/10.1038/nrg3522

Schork, A. J., Thompson, W. K., Pham, P., Torkamani, A., Roddey, J. C., Sullivan, P. F., … Andreassen, O. A. (2013). All SNPs are not created equal: Genome-wide association studies reveal a consistent pattern of enrichment among functionally annotated SNPs. *PLoS Genetics*, 9(4), e1003449. https://doi.org/10.1371/journal.pgen.1003449

Shao, H., Burrage, L. C., Sinasac, D. S., Hill, A. E., Ernest, S. R., O'Brien, W., … Daly, M. J. (2008). Genetic architecture of complex traits: Large phenotypic effects and pervasive epistasis. *Proceedings of the National Academy of Sciences*, 105(50), 19910–19914. https://doi.org/10.1073/pnas.0810388105

Siddle, H. V., Kreiss, A., Tovar, C., Yuen, C. K., Cheng, Y., Belov, K., … Skjødt, K. (2013). Reversible epigenetic down-regulation of MHC molecules by devil facial tumour disease illustrates immune escape by a contagious cancer. *Proceedings of the National Academy of Sciences*, 110(13), 5103–5108. https://doi.org/10.1073/pnas.1219920110

Simonson, T. S., Yang, Y., Huff, C. D., Yun, H., Qin, G., Witherspoon, D. J., … Prchal, J. T. (2010). Genetic evidence for high-altitude adaptation in Tibet. *Science*, 329(5987), 72–75. https://doi.org/10.1126/science.1189406

Skotte, L., Korneliussen, T. S., & Albrechtsen, A. (2012). Association testing for next-generation sequencing data using score statistics. *Genetic Epidemiology*, 36(5), 430–437. https://doi.org/10.1002/gepi.21636

Sulem, P., Gudbjartsson, D. F., Stacey, S. N., Helgason, A., Rafnar, T., Magnusson, K. P., … Jakobsdottir, M. (2007). Genetic determinants of hair, eye and skin pigmentation in Europeans. *Nature Genetics*, 39(12), 1443–1452. https://doi.org/10.1038/ng.2007.13

Turner, S. D. (2014). qqman: An R package for visualizing GWAS results using QQ and manhattan plots. *BioRxiv*, 005165.

Wang, Y., McKay, J. D., Rafnar, T., Wang, Z., Timofeeva, M. N., Broderick, P., … Lloyd, A. (2014). Rare variants of large effect in BRCA2 and

CHEK2 affect risk of lung cancer. *Nature Genetics*, *46*(7), 736–741. https://doi.org/10.1038/ng.3002

Wang, J., Syrett, C. M., Kramer, M. C., Basu, A., Atchison, M. L., & Anguera, M. C. (2016). Unusual maintenance of X chromosome inactivation predisposes female lymphocytes for increased expression from the inactive X. *Proceedings of the National Academy of Sciences*, *113*(14), E2029–E2038. https://doi.org/10.1073/pnas.1520113113

Wellenreuther, M., & Hansson, B. (2016). Detecting polygenic evolution: Problems, pitfalls, and promises. *Trends in Genetics*, *32*(3), 155–164. https://doi.org/10.1016/j.tig.2015.12.004

Wells, K., Hamede, R. K., Kerlin, D. H., Storfer, A., Hohenlohe, P. A., Jones, M. E., & McCallum, H. I. (2017). Infection of the fittest: Devil facial tumour disease has greatest effect on individuals with highest reproductive output. *Ecology Letters*, *20*(6), 770–778. https://doi.org/10.1111/ele.12776

Wise, A. L., Gyi, L., & Manolio, T. A. (2013). eXclusion: Toward integrating the X chromosome in genome-wide association analyses. *The American Journal of Human Genetics*, *92*(5), 643–647. https://doi.org/10.1016/j.ajhg.2013.03.017

Wood, A. R., Esko, T., Yang, J., Vedantam, S., Pers, T. H., Gustafsson, S., … Amin, N. (2014). Defining the role of common variation in the genomic and biological architecture of adult human height. *Nature Genetics*, *46*(11), 1173–1186. https://doi.org/10.1038/ng.3097

Wright, B., Willet, C. E., Hamede, R., Jones, M., Belov, K., & Wade, C. M. (2017). Variants in the host genome may inhibit tumour growth in devil facial tumours: Evidence from genome-wide association. *Scientific Reports*, *7*(1), 423. https://doi.org/10.1038/s41598-017-00439-7

Xu, H., & Shete, S. (2005). Effects of population structure on genetic association studies. *BMC Genetics*, *7*(1), S109. https://doi.org/10.1186/1471-2156-6-S1-S109

Yang, J., Bakshi, A., Zhu, Z., Hemani, G., Vinkhuyzen, A. A., Lee, S. H., … Snieder, H. (2015). Genetic variance estimation with imputed variants finds negligible missing heritability for human height and body mass index. *Nature Genetics*, *47*(10), 1114–1120. https://doi.org/10.1038/ng.3390

Yang, J., Benyamin, B., McEvoy, B. P., Gordon, S., Henders, A. K., Nyholt, D. R., … Goddard, M. E. (2010). Common SNPs explain a large proportion of the heritability for human height. *Nature Genetics*, *42*(7), 565–569. https://doi.org/10.1038/ng.608

Yang, J., Ferreira, T., Morris, A. P., Medland, S. E., Madden, P. A., Heath, A. C., … Frayling, T. M. (2012). Conditional and joint multiple-SNP analysis of GWAS summary statistics identifies additional variants influencing complex traits. *Nature Genetics*, *44*(4), 369–375. https://doi.org/10.1038/ng.2213

Zhou, X., Carbonetto, P., & Stephens, M. (2013). Polygenic modeling with Bayesian sparse linear mixed models. *PLoS Genetics*, *9*(2), e1003264. https://doi.org/10.1371/journal.pgen.1003264

Zhou, X., & Stephens, M. (2012). Genome-wide efficient mixed-model analysis for association studies. *Nature Genetics*, *44*(7), 821–824. https://doi.org/10.1038/ng.2310

SUPPORTING INFORMATION

Additional supporting information may be found online in the Supporting Information section at the end of the article.